ChemBioChem

Research Article
doi.org/10.1002/cbic.202401041

Chemistry Europe
European Chemical Societies Publishing

www.chembiochem.org

VIP *Very Important Paper*

A Practical Approach for Polarity and Quantity Controlled Assembly of Membrane Proteins into Nanoliposomes

Shiwei Zhang,[a] Peng Lin,[a, b] Futa Komatsubara,[b] Eiji Nakata,[a, b] and Takashi Morii*[a, c]

Biological membranes achieve selectivity and permeability through protein transporters and channels. The design of artificial compartments with permeable membranes is essential to facilitate substrate and product transfer in enzymatic reactions. In this study, an *E. coli* outer membrane protein OmpF fused to a modular adaptor was integrated onto a DNA origami skeleton to control the number and polarity of the OmpF trimer. DNA origami skeleton-guided nanoliposomes reconstituted with functional OmpF exhibit pH-responsiveness and size-selective permeability. This approach highlights the potential to construct artificial compartments that incorporate membrane proteins of defined number and polarity, allowing tunable substrate fluxes.

Introduction

Biological membranes serve as excellent separators by providing both controlled permeability and precise solute selectivity, which is attributed to specific membrane protein channels.[1] These channels possess unique pore geometries that are critical for the targeted separation of small molecules essential for cellular functions.[2–5] Some membrane proteins, such as porins, are constantly open, allowing non-selective molecule diffusion, while others open in response to external stimuli such as ions, temperature, or voltage changes. Reconstitution of these membrane proteins into lipid membranes of liposomes or polymersomes of various compositions and sizes has been reported.[6] For example, the outer membrane protein OmpF, a highly abundant trimeric porin of *E. coli* that facilitates general diffusion and is critical for the transport of antibiotics and colicins across the outer membrane,[7] has been used extensively in the synthesis of artificial filters,[8] sensors[9] and reactors.[10] The dimensions of the pore formed by the trimer of OmpF are approximately 7×11 Å, allowing the passage of molecules smaller than 500 Da.[11] When solubilized with detergents, OmpF can be reconstituted into artificial bilayers and retains its functionality as a trimeric ion-conducting porin with the same properties as its in vivo function.[12] However, achieving precise control over the number and polarity of these membrane proteins in lipid membranes of artificial compartments remains a challenge.

Rationally designed DNA nanoscaffolds have been decorated with lipid molecules at specific positions on their surfaces, enabling the construction of artificial membranes.[13–15] Advances in various assembly methods allow precise placement of proteins of interest (POIs) on DNA scaffolds[16] including DNA hybridization with covalently conjugated POIs[17] and noncovalent interactions such as biotin-avidin,[18,19] antibody-antigen[20,21] and DNA-binding proteins.[22] These methods provide flexible and reversible binding, but often result in low assembly yields. Our group has developed a modular adaptor method using sequence-specific DNA-binding proteins (zif268, AZP4, GCN4) and protein tags (SNAP-tag, Halo-tag, CLIP-tag) to precisely position proteins on DNA scaffolds in nearly quantitative yields.[23–26] This approach achieves high binding efficiencies, precise control of the number of proteins on the scaffold, and minimal interference with protein activity. Recently, we reported a DNA origami skeleton-guided liposome embedded with OmpF that exhibited a size-selective molecular transport function as an artificial compartment. The artificial compartment transported ions and molecules with a molecular weight below 600 Da.[27]

In this study, we designed a modular adaptor (ZF-SNAP)-fused OmpF for assembly onto the DNA origami skeleton constructed in our previous work.[27] This facilitated precise control over the number and polarity of ZF-SNAP-OmpF (ZSO) within the membrane of artificial compartments. After expression and purification, ZSO was refolded into lipids. The functional state of ZSO was confirmed by fluorescence microscopy, where a pH-sensitive fluorophore located on the internal DNA origami skeleton within the artificial compartments showed a response to pH changes in the external buffer. In addition, the size-dependent permeability of ZSO was investigated by introducing DNA intercalators of different molecular weights (EtBr, SYBR Green II, and GelRed). These intercalators either

[a] Dr. S. Zhang, Dr. P. Lin, Prof. E. Nakata, Prof. T. Morii
Institute of Advanced Energy, Kyoto University
Uji, Kyoto, 6110011 (Japan)
E-mail: morii.takashi.68s@st.kyoto-u.ac.jp

[b] Dr. P. Lin, F. Komatsubara, Prof. E. Nakata
Department of Fundamental Energy Science, Graduate School of Energy Science,Kyoto University
Yoshida, Sakyo-ku, Kyoto 6068501 (Japan)

[c] Prof. T. Morii
Department of Health and Nutrition, Kyoto Koka Women's University
Ukyo-ku, Kyoto 615-0882 (Japan)

Supporting information for this article is available on the WWW under https://doi.org/10.1002/cbic.202401041

passed through or were blocked by the resulting pore of the ZSO trimer, allowing selective binding to the DNA origami skeleton inside the liposomes. Interestingly, we found that when the molecular weight of the DNA intercalator was around 450 Da, its rate of transfer into the interior of the nanoliposome increased with increasing number of OmpF inserted into the liposome. This observation suggests that this method has the potential to regulate the substrate exchange rate in the construction of artificial compartments.

Results and Discussion

Anchoring of the Membrane Protein ZF-SNAP-OmpF (ZSO) on the DNA Origami Skeleton

To specifically locate a membrane protein to the wireframe DNA origami skeleton (WS), the membrane protein OmpF was genetically fused to the adaptor ZF-SNAP, which consists of both the DNA binding protein zif268 and a self-ligating protein tag SNAP-tag at the N-terminal, through a flexible GGS linker to yield ZSO (Figure 1a and Figure S1). To assemble the membrane protein, the DNA origami skeleton was designed according to our previous work.[27] A total of three binding sites for the ZF-

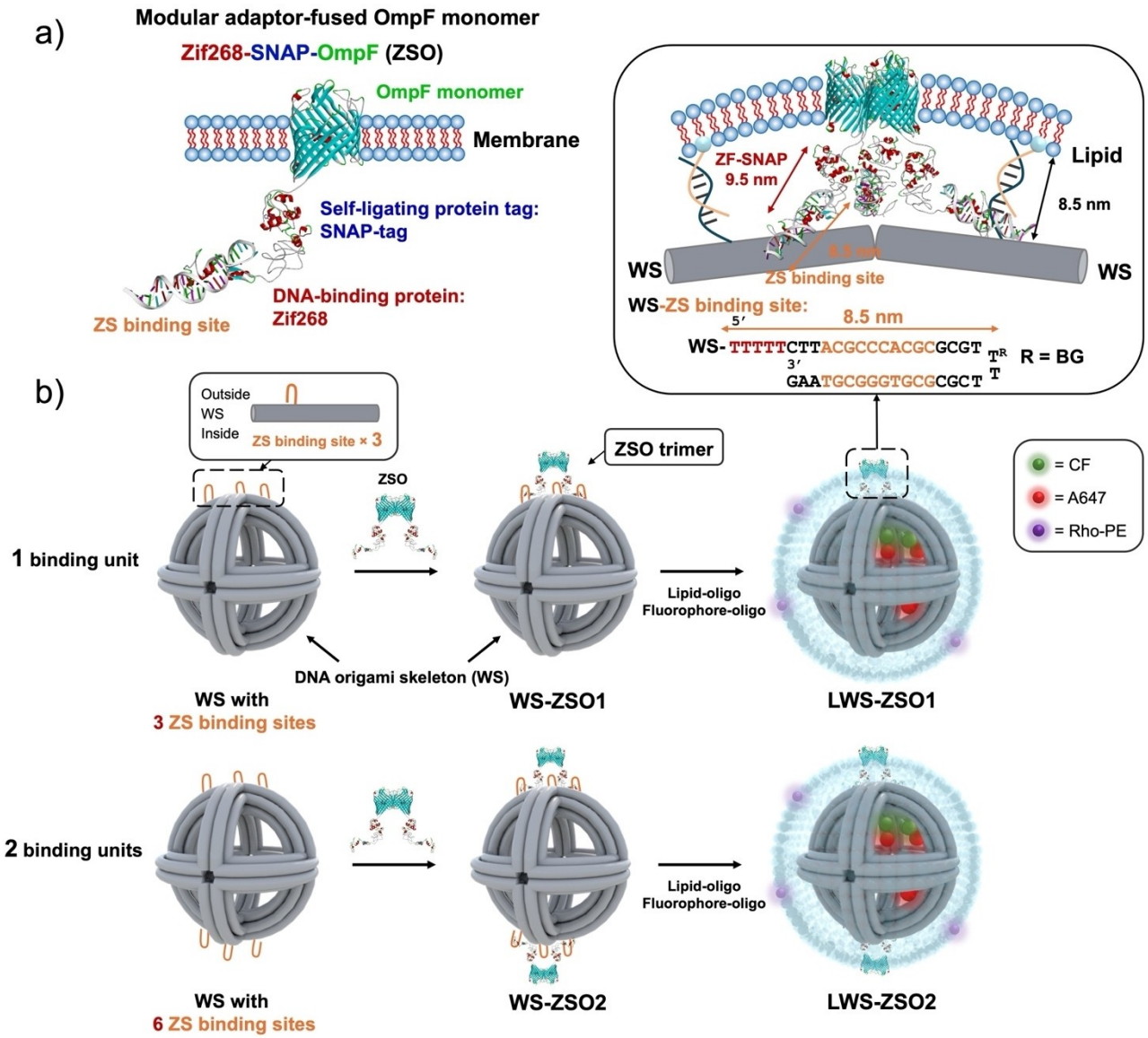

Figure 1. Design of modular adaptor-fused OmpF and binding sites on a DNA origami skeleton. (a) Illustrations showing the structure of the modular adaptor-fused OmpF monomer (ZSO). The modular adaptor-fused OmpF consists of the DNA-binding protein zif268, the self-ligating protein tag SNAP-tag and the membrane protein OmpF. (b) Schematic representation of the binding unit for ZSO assembly on the DNA skeleton (designed diameter of 58 nm). One binding unit contains three ZS binding sites, allowing the assembly of one ZSO trimer. WS-ZSO1 contains one binding unit, allowing assembly of a ZSO trimer, while WS-ZSO2 has two binding units at equatorial poles, allowing assembly of two ZSO trimers. After assembly with ZSO, lipidated ODN was attached to WS in a surfactant solution and combined with surfactant-lipid micelles to form liposomes (designed diameter of 80 nm) around WS (LWS-ZSO1 and LWS-ZSO2) by dialysis to remove excess surfactant.

SNAP adaptor were designed as the binding unit for assembly with the ZSO trimer (Figure 1b) to prepare WS containing either one or two binding units. The number of parents OmpF inserted into liposomes was found to be three trimers per WS liposome (LWS) in our previous study.[27] The modular adaptor was designed to regulate the number of ZSO on LWS. The binding sites for ZSO were designed as hairpin DNA sequences. These sequences consist of the zif268-specific binding sequence in the stem region and the tag substrate BG in the loop region. In previous work, we determined that the diameter of LWS is approximately 76 nm, while the diameter of WS is 56 nm, resulting in a gap of 8.5 nm between the liposome and WS. To provide flexibility for ZSO binding and to adjust the distance between the N-terminal portion of OmpF and the edge of the WS surface, the hairpin DNA sequences were extended to a total length of 8.5 nm. Importantly, the modular adaptor is non-hydrophobic, which is critical for the polarity control of ZSO. Since it cannot spontaneously cross the membrane, it dictates that the membrane protein can only be inserted into the liposome in a specific orientation, thereby ensuring effective regulation of the number and polarity of OmpF trimers within the liposome membrane. This design feature provides a basis for the construction of artificial compartments with precisely controlled membrane protein properties. After ZSO binds to the DNA skeleton WS through the modular adaptor ZS, it can only be inserted into the membrane of the subsequently constructed liposome with a unique polarity, allowing control over the orientation of OmpF with respect to the DNA skeleton WS (Figure 1b).

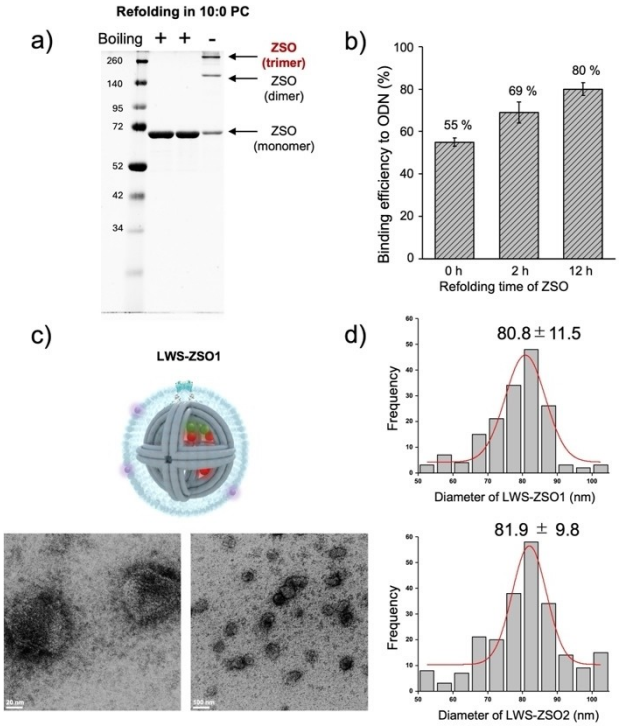

Figure 2. (a) The 12% SDS-PAGE image of purified ZSO (over 95% purity) and ZSO refolded in 10:0 PC. In 6 M urea, ZSO exists as a monomer. After refolding in 10:0 PC without heat denaturation, it appears as a trimer on SDS-PAGE. (b) The binding efficiency of ZSO and ODN-BG increases with the refolding time of ZSO, reaching a maximum binding efficiency of up to 80% after 12 hours of refolding. (c) TEM images of LWS-ZSO-1. Scale bar: 20 nm or 100 nm. (d) Histograms show that the diameters of LWS-ZSO1 and LWS-ZSO2 measured from TEM images are 80.8 ± 11.5 nm (N = 182) and 81.9 ± 9.8 nm (N = 242), respectively.

Preparation and Characterization of OmpF Anchored Nanoliposomes

Since the expressed ZSO had very low solubility in the lysis buffer, urea was used to denature the protein to prevent digestion and improve solubility. Increasing the urea concentration in the lysis buffer improved the solubility of ZSO, with optimal solubility observed at 6 M urea (Figure S3). Inclusion body pellets of ZSO were solubilized in 6 M urea and 20 mM Tris-HCl, pH 8.0. Ni/NTA affinity purification was performed on an AKTA system using HisTrap HP columns. The purity of ZSO with the expected molecular weight (71.3 kDa) and purity $>$98% is shown in Figure 2a.

After purification, ZSO was refolded by dilution in large unilamellar liposome (LUV) formed by 5 mM 1,2-dioleoyl-sn-glycero-3-phosphocholine (DOPC) or 1,2-didecanoyl-sn-glycero-3-phosphocholine (10:0 PC) in folding buffer containing 1 M urea and 20 mM Tris-HCl buffer (pH 8.0). SDS-PAGE analysis was used to determine the fraction of protein that refolded under these conditions (Figure S4a). When ZSO was solubilized in SDS and then boiled, ZSO lost its native β-content and migrated to its expected molecular weight on polyacrylamide gels.[28] Non-boiled samples of folded ZSO retained a high content of β-structure as well as its activity to form oligomers and migrated to a different position than the unfolded form. Therefore, SDS-PAGE was used to distinguish between the folded and unfolded populations. From the SDS-PAGE shown in Figure 2a and Figure S4b, when incubated with a 10:0 PC LUVs, over 75% of ZSO folded into trimers, 15% formed dimers, and 10% remained unfolded. In contrast, no folding was observed when incubated with DOPC LUVs and Tris-HCl buffer. As a control, native OmpF and ZSO were also expressed and refolded in 5 mM 10:0 PC in folding buffer. SDS-PAGE analysis revealed that over 80% of native OmpF folded into trimers, 12% formed dimers, while 8% remained unfolded (Figure S5, left). These results strongly suggest that the refolding of ZSO is dependent on acyl chain length and bilayer thickness.[29]

The DNA binding ability of ZSO to the ODN containing its target zif268-binding sequence modified by a SNAP-tag substrate benzylguanine (ODN-BG) (Figure S2c) was analyzed by gel mobility assay (Figure S6). The formation of a covalent bond between ZSO (100 nM) and ODN-BG (1 μM) resulted in a slower migrating band compared to free ZSO. ZS-XR (100 nM), a ZS modular adaptor fused to xylose reductase previously reported by our group,[25] and ZS-XR modified ODN-BG formed by ZS-XR (100 nM) and ODN-BG (1 μM) were used as control samples. By comparing the band intensity observed between free ZS-XR and ZS-XR modified ODN-BG, it was estimated that over 95% of the ZS-XR formed the complex. At 6 M urea, only 55 ± 2% of the unfolded ZSO formed a complex with ODN-BG, consistent with

previous reports (Figure 2b). Similarly, Gautier *et al.* reported that the urea concentration required for 50% inactivation of the SNAP-tag ($[urea]_{1/2}$) was 6.3 ± 0.1 M.[30] However, after refolding for 2 hours in folding buffer (1 M urea and 20 mM Tris-HCl buffer, pH 8.0) containing 5 mM 10:0 PC LUVs, the binding yield increased to 69 ± 6%. Furthermore, the yield reached 80 ± 3% after 12 hours of incubation. The observed binding yield of ZSO, which was lower than the 95% observed for ZS-XR, could be attributed to the influence of urea on ZF-SNAP.

To assemble OmpF on the DNA origami skeleton, 20 nM WS with one or two binding units was incubated with 1500 nM ZSO at 4 °C for 2 hours. Purification by gel filtration (TOYOPEARL HW55F) removed unbound proteins, resulting in purified ZSO-modified DNA skeleton (WS-ZSO1 and WS-ZSO2). Due to the relatively low molecular weight of ZSO compared to that of WS, no significant band shift was observed for ZSO-modified WS on the agarose gel after binding with ZSO (Figure S7). The binding of ZSO to WS was observed in the AFM image (Figure S8). However, due to the 3D shape of WS, it was difficult to accurately calculate the actual number of ZSO molecules bound to the target sites of WS based on the AFM image. This will be discussed in a later section.

The WS-ZSO was combined with DOPC containing 0.8% rhodamine-modified lipid to reconstitute a lipid bilayer by dialysis for 48 hours. The dialyzed solution was then loaded onto an iodixanol gradient and ultracentrifuged to isolate liposome-coated LWS-ZSO1 and LWS-ZSO2 (Figure S9). The isolated LWS-ZSO1 and LWS-ZSO2 fractions were then analyzed by TEM (Figure 2c, Figure S10). The outer membrane diameter of LWS-ZSO1 and LWS-ZSO2 was determined by TEM images to be 80.8 ± 11.5 nm and 81.9 ± 9.8 nm, respectively, each having a diameter similar to the designed diameter (80 nm)[27] (Figure 2d).

Microscopic Characterization of OmpF Anchored to the Skeleton of Liposomes

The LWS-ZSO compartment was immobilized on a slide coated with biotin-BSA and streptavidin.[27] At pH 8.0, strong spots of fluorescence emission were observed from the CF fluorophore located within LWS, LWS-ZSO1 and LWS-ZSO2.[27,31] The overlapping of fluorescence signals from CF, Rho, and A647 at the same positions in the fluorescence image confirmed the successful and nearly quantitative construction of LWS-ZSO1 (Figure 3a). When the external buffer was changed from pH 8.0 to pH 6.0, 42 ± 3% of LWS-ZSO1 showed a decrease in CF fluorescence intensity to 33 ± 3% of the initial value (Figure 3b and S11, N = 82). For LWS-ZSO2, which contains two binding units for ZSO, the decrease in intensity was observed in 58 ± 5% of the liposomes (Figure 3c, 3d and S12, N = 74). This is in marked contrast to the result obtained for LWS in the absence of OmpF. In this case, the fluorescence intensity of the CF fluorophore within the LWS showed no significant change (Figure S13 and Table S3, N = 59). These results indicate the successful incorporation of ZSO into the nanoliposomes and

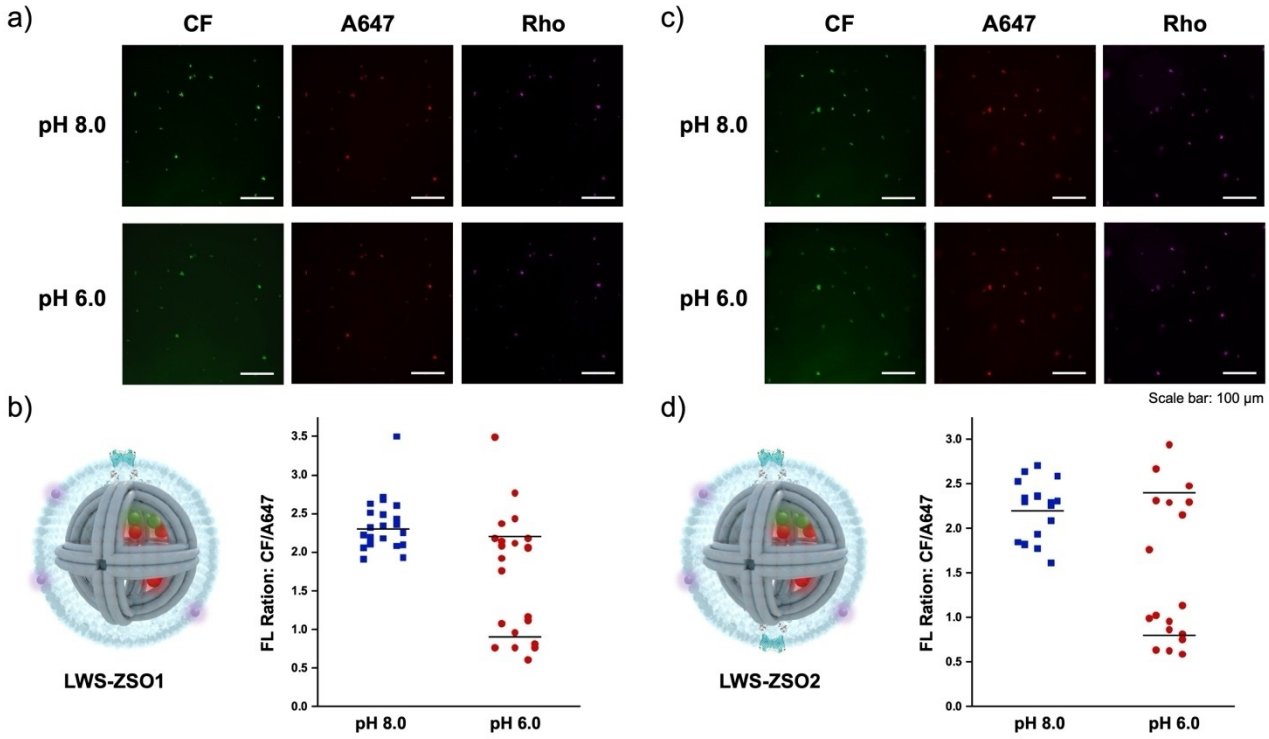

Figure 3. An illustration of buffer diffusion through the ZSO-embedded membrane of LWS-ZSO. Fluorescence images of LWS-ZSO1 (a) and LWS-ZSO2 (c) immobilized on a biotin-BSA and streptavidin-coated surface were taken at the CF channel, Rho channel, and A647 channel at pH 8.0 and 6.0, respectively. Scale bar: 100 μm. Plot of fluorescence intensity ratio (CF/A647) of individual LWS-ZSO1 (b) (N = 22) and LWS-ZSO2 (d) (N = 18) under each indicated pH condition.

demonstrate that the adaptor-fused membrane protein ZSO assembled on WS was reconstituted into the artificial LWS-ZSO compartments in an active form.

Evaluation of the Activity of Liposome-anchored OmpF using Intercalators

The size-dependent permeability of liposome- anchored OmpF was evaluated using DNA intercalators (EtBr, SYBR Green II, and GelRed) of different molecular weights (Figure S14). In our previous work, we reported that the average number of OmpF trimers inserted into LWS was 3.0 per compartment (LWS-O3).[27] Therefore, LWS-O3 was compared with LWS-ZSO containing one (LWS-ZSO1) or two binding units (LWS-ZSO2). Because the molecular weight of GelRed (985.3) is much larger than the cut-off of OmpF (500 Da),[11] the increase in GelRed fluorescence signal during incubation with liposome-coated WS is attributed to its binding to WS that is not fully encapsulated by the liposome (Figure 4a). This allowed us to calculate the encapsulation yield of LWS, LWS-ZSO1, LWS-ZSO2 and LWS-O3 by comparing the fluorescence intensity of GelRed at the same WS concentration. The encapsulation yields of LWS, LWS-O3, LWS-ZSO2, and LWS-ZSO1 are 89 ± 3%, 88 ± 4%, 92 ± 6%, and 90 ± 4%, respectively (Figure 4b and Figure S15). The lack of significant differences between them further demonstrates that this method is applicable to encapsulate the DNA skeleton with or without the anchored proteins. When the encapsulating liposomes were disrupted by adding SDS, the fluorescence intensity of GelRed binding with liposome-encapsulated WS (LWS-ZSO1, LWS-ZSO2, and LWS-O3) reached that of WS, confirming that each sample contains the same concentration of WS.

EtBr is smaller than GelRed with a molecular weight of 314.4, which allows it to rapidly pass through OmpF in the lipid membranes and bind to the DNA duplex of WS inside the liposome, as we have previously reported.[27] Here, the increase in EtBr fluorescence intensity can be used to determine the loading yield of ZSO to WS on the liposome (Figure 4c and 4d). After incubation with EtBr, the fluorescence intensity of EtBr with LWS increased by 12 ± 2% compared to the increase with WS, indicating that 88 ± 2% of LWS is well coated with liposomes. This result is consistent with the encapsulation yields estimated from the GelRed experiment above. The fluorescence intensity of EtBr with LWS-ZSO1 and LWS-ZSO2 increased by 48 ± 4% and 68 ± 2%, respectively, compared to its increase in WS. Considering that 12 ± 2% of the liposomes are not well coated, the loading yield of ZSO to one binding unit is 36 ± 2%, while its loading yield to two binding units is 56 ± 2%. These results are consistent with those observed by fluorescence microscopy (Figure 3). It can be calculated that with one binding unit (LWS-ZSO1), each liposome contains an average of 0.4 ± 0.03 ZSO trimers. For WS containing two binding units (LWS-ZSO2), loading of one or two ZSO trimers is possible. With a loading yield of 40%, the probability that only one ZSO trimer will bind to the two binding units is 48%, while the probability that two ZSO trimers will bind is 16%, resulting in a total probability of 64%. This calculation is close to the experimental result of 58 ± 5% (Figure 3d) and supports the estimation that each liposome contains an average of 0.8 ± 0.02 ZSO trimers when two binding units are present. The results with GelRed and EtBr shown above confirmed that the size-dependent permeability of ZSO in the membrane and fusing with the modular adaptor does not affect the intrinsic function of OmpF.

The cut-off of ZSO was further investigated with intercalators of similar molecular weight. SYBR Green II (molecular weight 454.6) and SYBR Green I (molecular weight 509.7). Interestingly, despite its molecular weight of less than 500, SYBR Green II could not rapidly pass through the OmpF-embedded membrane to bind to WS like EtBr (Figure 4e and Figure S16 and S17). In contrast, SYBR Green I did not pass through the OmpF-embedded membrane (less than 5%) (Figure S18). This result is consistent with previous reports that for small molecules with molecular weights above 480, approximately 90% of them are unable to pass through OmpF-embedded biomimetic membranes.[8]

Furthermore, the binding rate increased with the number of OmpF trimers on the liposome (Figure 4f and 4g). 10 nM SYBR Green II binds the internal WS of the liposome-encapsulated WS containing three native OmpF trimers (LWS-O3) at a rate similar to its binding rate to WS without liposome encapsulation, with $T_{1/2}$ of 31 ± 7 s and 12 ± 6 s, respectively, where $T_{1/2}$ is the time required for half saturation of fluorescence intensity (Figure 4f). In contrast, for LWS-ZSO containing one or two binding units with an average of 0.4 ± 0.03 OmpF trimers and 0.8 ± 0.02 OmpF trimers, the $T_{1/2}$ values were 112 ± 17 s (LWS-ZSO1) and 36 ± 12 s (LWS-ZSO2), respectively. Subsequently, $T_{1/2}$ values were measured with different numbers of OmpF at different concentrations of SYBR Green II ranging from 2.5 nM to 40 nM. The $T_{1/2}$ values increased as the number of OmpF trimers on the liposomes decreased and also increased as the concentration of SYBR Green II decreased (Figure 4g). The diffusion of EtBr into OmpF-embedded liposomes was also investigated. Since the molecular weight of EtBr is much smaller than the cut-off of OmpF, the binding rates observed for liposomes with different numbers of OmpF trimer (LWS-ZSO1, LWS-ZSO2 and LWS-O3) were similar to each other. As the EtBr concentration decreased from 100 nM to 10 nM, the $T_{1/2}$ values increased from 16 ± 4 s to 36 ± 7 s for LWS-ZSO1 (Figure S19). No significant changes were observed for LWS-ZSO2 and LWS-O3. These results suggest that by controlling the number of OmpF trimers on the liposome, it is possible to regulate the rate at which molecules of appropriate molecular weight, i.e. near the cut-off molecular weight, are transported through the liposome.

Conclusions

The bacterial outer membrane protein OmpF was fused to the modular adaptor ZF-SNAP (ZSO) to control the number and polarity of OmpF trimers within the membrane of liposomes with an internal DNA origami skeleton. Despite the effect of urea denaturation during the purification of ZSO, which resulted in incomplete recovery of SNAP-tag activity after

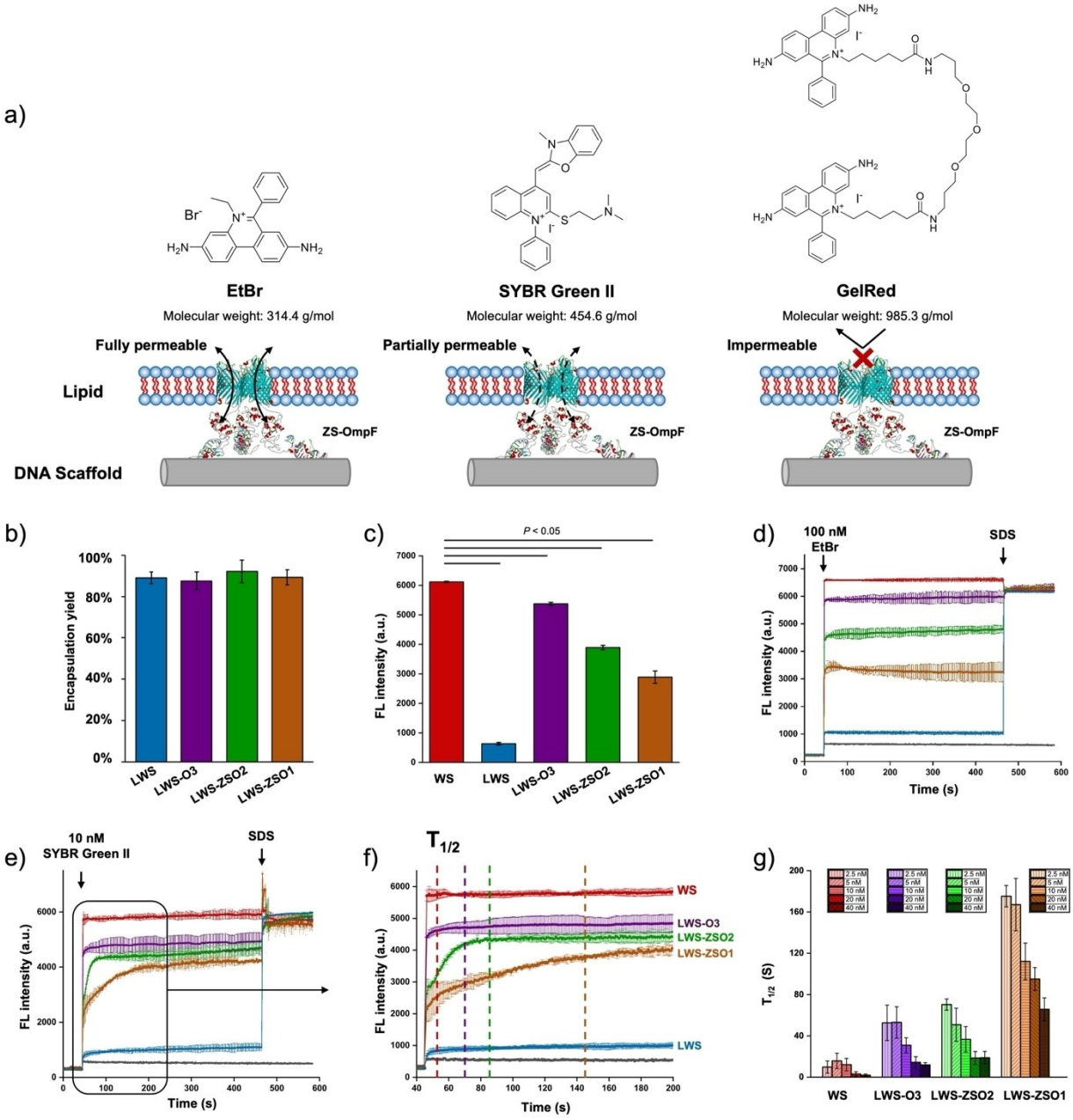

Figure 4. Size-dependent permeability of ZSO evaluated using DNA intercalators (EtBr, SYBR Green II, GelRed) of different molecular weights. (a) A scheme illustrates that the molecular cutoff size of OmpF is approximately 480, indicating that EtBr (molecular weight 314.4) can completely pass through OmpF and bind to the DNA duplex of WS. SYBR Green II (molecular weight 454.6) can partially and slowly pass through OmpF and bind to the DNA duplex of WS. In contrast, GelRed (molecular weight 985.3) is unable to pass through OmpF. (b) The encapsulation yields of LWS, LWS-ZSO1 and 2, and LWS-O3 were estimated using GelRed. The increase in GelRed fluorescence intensity can be attributed to the presence of incomplete liposomes, as GelRed is unable to pass through OmpF. (c) The binding yield of ZSO to WS was estimated from the fluorescence intensity of EtBr bound to the DNA duplex of WS. (d) The changes in fluorescence intensity of EtBr when mixed with WS (red), LWS (blue), LWS-O3 (purple), LWS-ZSO2 (green), and LWS-ZSO1 (brown), followed by the addition of SDS. After the addition of SDS, which disrupts the liposomes, the fluorescence intensity of EtBr reaches saturation, indicating that the WS concentrations of all samples are the same. (e) The changes in fluorescence intensity of SYBR Green II when mixed with WS (red), LWS (blue), LWS-O3 (purple), LWS-ZSO2 (green), and LWS-ZSO1 (brown), followed by the addition of SDS. (f) The magnified image shows that SYBR Green II can partially pass through OmpF, and the rate of passage increases as the number of OmpF trimers increases. The dashed line indicates the time when the fluorescence intensity reaches its maximum value. (g) $T_{1/2}$ values of WS (red), LWS (blue), LWS-O3 (purple), LWS-ZSO2 (green), and LWS-ZSO1 (brown) were measured at different concentrations of SYBR Green II ranging from 2.5 nM to 40 nM

refolding, ZSO still exhibited a loading yield of 42 ± 3% with a single binding unit (for one trimer) and 58 ± 5% with two binding units (for two trimers). As a result, liposome-coated WS with one binding unit for ZSO contained an average of 0.4 ± 0.03 OmpF trimers per nanoliposome, while those with two binding units contained an average of 0.8 ± 0.02 OmpF trimers per nanoliposome. Furthermore, the functionality of the membrane protein OmpF was confirmed by the response to external

pH and by the size-selective transport of DNA intercalators into the interior of the liposomes, showing that fusion with ZF-SNAP does not affect its function. Using the intercalators, faster transport kinetics were observed for the liposome compartments with more OmpF incorporated. By controlling the number of OmpF in the compartments, the transport kinetics of substrates or reaction intermediates can be regulated, which is of great importance for the regulation of enzyme reactions, especially cascade reactions, in the compartments. Although it is known that the orientation of OmpF does not significantly affect its function of transporting molecules and ions, using OmpF as a first example opens further possibilities for the construction of a wider range of modular adaptor-fused membrane proteins. This work provides a potential approach to control the number and polarity of channels in artificial compartments, providing insight for future developments in membrane protein engineering.

Experimental Section

Materials: M13 single-stranded viral DNA (p7308) was purchased from Guild Biosciences. BG-GLA-NHS (S9151S) and bovine serum albumin (BSA, BS9000S) were purchased from New England Biolabs. Purified oligonucleotides for DNA origami staple strands, oligonucleotide primers, and all other oligonucleotides were purchased from Sigma-Aldrich (St. Louis, MO), Japan Bio Services Co., LTD (Saitama, Japan) or Thermo Fisher Scientific (Tokyo, Japan). Escherichia coli (*E. coli*) BL21(DE3) competent cells were purchased from Thermo Fisher Scientific (Tokyo, Japan). All other chemicals and reagents were purchased from Wako Chemicals (Tokyo, Japan) or Nacalai Tesque (Kyoto, Japan). Mini Elute Gel Extraction Kit was from QIAGEN (Tokyo, Japan). HisTrap HP column (5 mL) and Sephacryl S-400 were purchased from Cytiva Japan Inc. (Tokyo, Japan). PrimeSTAR HS DNA polymerase, T4 DNA ligase, and E. coli DH5α competent cells were purchased from TaKaRa Bio Inc. (Shiga, Japan). TOYOPEARL HW-55F was from Tosoh Corporation (Tokyo, Japan). Ultrafree-MC–DV column was from Merckmillipore (Darmstadt, Germany). Low binding microtube (BT-150L, 1.5 mL, non-pyrogenic & RNase-/DNase-free) was purchased from Ina OPTIKA CO., LTD (Osaka, Japan).

Construction of a vector encoding ZSO: The OmpF gene in pET-30a-OmpF and a modular adaptor ZS gene in pET-30a-ZS-XR[25] were amplified by PCR using the primer pairs shown in Table 1. The histidine tag was introduced at the N-terminus of ZF-SNAP. The PCR products and pET-30a were digested with *Nde* I and *Hind* III. They were run on a 1% agarose gel in 1xTAE buffer and were purified by a Mini Elute Gel Extraction Kit, separately. These products were incubated with T4 DNA ligase and then transformed into *E. coli* DH5α competent cells for amplification. The purity and sequence of the vector encoding ZSO was confirmed and transformed into *E. coli* BL21 (DE3) competent cells for protein expression.

Expression and purification of ZSO: ZSO was expressed in LB medium supplemented with 30 μg/mL kanamycin in shake flasks. Cells were grown to an optical density at 600 nm of 0.6–0.8 at 37 °C and 250 rpm before protein expression was induced with isopropyl β-D-1-thiogalactopyranoside (IPTG) to a final concentration of 0.5 mM. Protein expression was allowed to proceed for 24 h at 18 °C and 250 rpm. Cells were harvested by centrifugation at 4000×g for 15 min at 4 °C. A 6 M urea solution (10 mM Tris-HCl, pH 8.0, 20 mL) was added to resuspend the cell pellet. The soluble fraction of the cell lysis containing ZSO was applied to a HisTrap HP column in a buffer of 20 mM Tris-HCl, pH 7.5, 0.3 M NaCl, 5 mM β-mercaptoethanol, 6 M urea and eluted by a gradient of imidazole concentration from 10 mM to 250 mM. The purity of ZSO was verified by SDS-PAGE. The major band in SDS-PAGE corresponded to the molecular weight of ZSO (71.3 kDa) with over 95% purity (Figure 2a).

Refolding of ZSO: ZSO was refolded by dilution of ZSO in 6 M urea in 5 mM LUVs formed from 1,2-didecanoyl-sn-glycero-3-phosphocholine (10:0 PC) in folding buffer (1 M urea and 20 mM Tris-HCl buffer, pH 8.0) to a final concentration of 4 μM protein at 30 °C for 15 h. After refolding, the buffer was changed to 1% OG in 20 mM Tris-HCl buffer through a 50 kDa Amicon Ultra tube.

Preparation of DNA origami skeletons: A solution (50 μL) containing M13 p7308 (30 nM) and mixture of staple DNA strands (400 nM) in a buffer (pH 8.0) containing 5 mM Tris-HCl, 1 mM EDTA, 14 mM $MgCl_2$ was incubated at 80 °C for 5 min, cooled to 65 °C at 5 min/°C, incubated at 65 °C for 20 min, cooled to 25 °C at 20 min/°C, and further cooled to 4 °C using a thermal cycler (C1000 Thermal Cycler, BioRad). The sample was purified by gel filtration using an Ultrafree-MC–DV column to remove excess staple strands, and the buffer was changed to 40 mM Tris-HCl and 12.5 mM $MgCl_2$, to remove EDTA. The concentration of DNA skeleton WS was quantified by absorbance at 260 nm (Nanodrop, Thermo Fisher Scientific Inc.) using the extinction coefficient of WS ($1.17\times10^8\ M^{-1}cm^{-1}$).

Preparation of ZSO-assembled DNA skeletons : DNA skeletons WS containing the binding sites (hairpin DNA) with BG-GLA-NHS modification were constructed for ZSO attachment (Table S4). 20 nM DNA skeleton with binding sites was incubated with 1500 nM ZSO in a buffer (pH 8.0) containing 40 mM Tris-HCl and 12.5 mM $MgCl_2$, 5 mM β-mecaptoethanol, 0.002% Tween20 and 1 μM $ZnCl_2$ at 4 °C for 15 h. The mixture was purified by gel filtration (500 μL in volume of Toyopearl HW55F) on an Ultrafree-MC–DV column with a buffer (pH 8.0) containing 40 mM Tris-HCl and 12.5 mM $MgCl_2$ to remove excess unbound proteins.

Agarose gel electrophoresis: Samples were run on a 1.5% agarose gel in 0.5×TBE containing 10 mM $MgCl_2$ at 50 V for 2 h in the cold storage chamber. The gel was visualized by using ChemiDoc™ MP (Bio-Rad) under the EtBr channel.

Table 1. List of primers used for construction of the vector encoding ZSO.

primers	Sequence (from 5′ to 3′)
F-His-ZF-SNAP	CATATGGGGTCCTCCCACCATCATCATCATCATAGCAGCGGCCTGGAAGTTCTGTTCCAGGGGCCCATGAAAACCGGGGAGAAACGCCCG
F-GGS3GG-OmpF	CATCGTCTGGGTAAACCGGGTCTGGGAGGCGGCAGCGGCGGCAGCGGCGGCAGCGGCGGCGAAATCTATAACAAAGATGGCAAC
R-ZF-SNAP-GGS3GG	GTTGCCATCTTTGTTATAGATTTCGCCGCCGCTGCCGCCGCTGCCGCCGCTGCCGCCTCCCAGACCCGGTTTACCCAGACGATG
R-OmpF	CTCGAGTTAGAACTGGTAAACGATACCCAC

Preparation of DNA skeleton-guided liposomes: A solution containing 10 nM WS-ZSO, 240 nM CF-modified DNA and 240 nM A647 modified DNA, 500 nM lipid-modified DNA and 1% OG in 40 mM Tris-HCl, 14 mM $MgCl_2$, 10 mM NaCl was incubated at 35 °C for 1 hour. To form DNA skeleton-guided liposomes, 80 μL of 5 mM DOPC (0.8% Rho-PE) was added to 160 μL of 10 nM lipid, CF and A647 labeled WS-ZSO to give a total volume of 240 μL and the solution was shaken for 30 minutes at room temperature. The solution was diluted with 240 μL of 40 mM Tris-HCl, 14 mM $MgCl_2$, 10 mM NaCl buffer containing 0.67% OG and dialyzed overnight against 2 L buffer. 190 μL of the recovered solution was mixed with 110 μL of 54% iodixanol in 1× hydration buffer and added to the bottom of a centrifuge tube (11×34 mm, Beckman Coulter Inc.). Six additional layers of 0 to 18% iodixanol in buffer were added to the centrifuge tube (Figure S9). The tube was spun in an MLA-130 rotor (Beckman Coulter Inc.) at 150,000×g at 4 °C for 5 hours, and the fractions (55 μL per fraction) were collected.

AFM imaging: The purified WS-ZSO was applied to a mica surface (1.5 mm diameter) and allowed to adsorb for 5 minutes at room temperature. The sample was then washed three times with a buffer (pH 8.0) containing 40 mM Tris-HCl and 14 mM $MgCl_2$. The sample was scanned in solution in tapping mode using a fast scanning AFM system (Nano Live Vision, RIBM Co. Ltd, Tsukuba, Japan) with a silicon nitride cantilever (Olympus BL-AC10DS–A2).

TEM imaging: LWS-ZSO solution (2 μL) was applied to a glow-discharged TEM grid and incubated for 3 minutes. Excess sample was removed with filter paper and the grid was incubated with 2% phosphotungstic acid (2 μL) for 2 minutes. Excess phosphotungstic acid was then removed with filter paper. The samples were analyzed using a TEM microscope (JEOL JEM-1400).

Fluorescence microscopy analysis of external buffer pH change: The LWS-ZSO containing biotin-modified lipid was loaded onto a Ibidi μ-Slide I 0.2 Luer, ibiTreat pretreated with biotinylated bovine serum albumin and neutravidin, adsorbed for 15 minutes at room temperature, and then washed three times with 50 mM phosphate buffer (pH 8.0). The fluorescence of the samples was observed using an IX-81 fluorescence microscope (Olympus) equipped with a 20× objective lens and a Xe lamp. Fluorescence images were captured with an electron multiplier CCD camera (Hamamatsu Photonics K.K.) at room temperature. After the fluorescence of CF, Rho and A647 were monitored sequentially (image: pH 8.0), the sample was washed with 50 mM phosphate buffer (pH 6.0) to change the pH of the external buffer. The fluorescence images of them were taken again at the same position (image: pH 6.0).

Fluorescence measurement to evaluate encapsulation efficiency: The fluorescence intensity of GelRed was measured at 25 °C using an Infinite 200 PRO microplate reader (TECAN, Austria, GmbH) with excitation at 490 nm and emission at 590 nm. WS, LWS, LWS-O3, LWS-ZSO1 or LWS-ZSO2 (1 nM) was added to a 96-well plate (90 μL) with GelRed (100 nM). After 15 minutes, 0.1% SDS was added to disrupt the liposomes.

Fluorescence measurements to analyze the binding kinetics of SYBR Green II and EtBr to WS: The fluorescence intensity of EtBr was measured at 25 °C using an Infinite 200 PRO microplate reader (TECAN, Austria, GmbH) with excitation at 485 nm and emission at 585 nm, and the fluorescence intensity of SYBR Green II was measured with excitation at 485 nm and emission at 530 nm. A solution (90 μL) containing WS, LWS, LWS-O3, LWS-ZSO1 or LWS-ZSO2 (1 nM) was added to a 96-well plate. In a subsequent experiment, after 40 cycles (1 second per cycle), 10 μL of solution containing intercalator was added using a injector. After 600 cycles, 5 μL of 1% SDS was injected using another injector to disrupt the liposomes.

Acknowledgements

This work was supported by JSPS KAKENHI Grant Numbers 23H02083, 23K26776 (T.M.), 24K01629, 24H01129 (E.N.), and 24K17787 (P.L.), Japan. This work acknowledges the Collaboration Program of the Laboratory for Complex Energy Processes, Institute of Advanced Energy, Kyoto University. This work also acknowledges Kyoto University Educational Research Foundation. The TEM measurements in this work were supported by the Analysis and Development System for Advanced Materials (ADAM) of RISH, Kyoto University, as a collaborative program, or the Kyoto University Nano Technology Hub in the "Nanotechnology Platform Project" sponsored by the Ministry of Education, Culture, Sports, Science and Technology (MEXT), Japan. S. Zhang would like to acknowledge the China Scholarship Council (CSC) for the PhD scholarship.

Conflict of Interests

The authors have no conflicts of interest directly relevant to the content of this article.

Data Availability Statement

The data that support the findings of this study are available in the supplementary material of this article.

Keywords: DNA origami · liposomes · modular adaptor · membrane transporter · size exclusion transport

[1] H. Park, J. Kamcev, L. Robeson, M. Eilmelech, B. Freeman, *Science* **2017**, *356*, eaab0530.
[2] M. Kumar, M. Grzelakowski, J. Zilles, M. Clark, W. Meier, *Proc. Nat. Acad. Sci.* **2007**, *104*, 20719.
[3] M. Kumar, J. Habel, Y. Shen, W. Meier, T. Walz, *J. Am. Chem. Soc.* **2012**, *134*, 18631.
[4] R. Chowdhury, T. Ren, M. Shankla, K. Decker, M. Grisewood, J. Prabhakar, C. Baker, J. Golbeck, A. Aksimentiev, M. Kumar, C. Maranas, *Nat. Commun.* **2018**, *9*, 3661.
[5] T. Ren, M. Erbakan, Y. Shen, E. Barbieri, P. Saboe, H. Feroz, H. Yan, S. McCuskey, J. F. Hall, A. Schantz, G. C. Bazan, P. Bulter, M. Grzelakowski, M. Kumar, *BioSystems* **2017**, *1*, 1700053.
[6] L. Tamm, H. Hong, B. Liang, *Biochimica et Biophysica Acta (BBA) - Biomembranes* **2004**, *1666*, 250.
[7] S. W. Cowan, T. Schirmer, G. Rummel, M. Steiert, R. Ghosh, R. A. Pauptit, J. N. Jansonius, J. P. Rosenbusch, *Nature* **1992**, *358*, 727.
[8] Y. M. Tu, W. Song, T. Ren, Y. Shen, R. Chowdhury, P. Rajapaksha, T. E. Culp, L. Samineni, C. Lang, A. Thokkadam, D. Carson, Y. Dai, A. Mukthar, M. Zhang, A. Parshin, J. N. Sloand, S. H. Medina, M. Grzelakowski, D. Bhattacharya, W. A. Phillip, E. D. Gomez, R. J. Hickey, Y. Wei, M. Kumar, *Nat. Mater.* **2020**, *19*, 347.
[9] G. Ghale, A. G. Lanctôt, H. T. Kreissl, M. H. Jacob, H. Weingart, M. Winterhalter, W. M. Nau, *Angew. Chem. Int. Ed.* **2014**, *53*, 2762.
[10] C. Edlinger, T. Einfalt, M. Spulber, A. Car, W. Meier, C. G. Palivan, *Nano Lett.* **2017**, *17*, 5790.
[11] G. Kefala, C. Ahn, M. Krupa, L. Esquivies, I. Maslennikov, W. Kwiatkowski, S. Choe, *Protein Sci.* **2010**, *19*, 1117.
[12] C. Nardin, S. Thoeni, J. Widmer, M. Winterhalter, W. Meier, *Chem. Commun.* **2000**, *15*, 1433.
[13] S. D. Perrault, W. M. Shih, *ACS Nano* **2014**, *8*, 5132.
[14] Y. Yang, J. Wang, H. Shigematsu, W. Xu, W. M. Shih, J. E. Rothman, C. Lin, *Nat. Chem.* **2016**, *8*, 476.

[15] X. Bian, Z. Zhang, Q. Xiong, P. D. Camilli, C. Lin, *Nat. Chem. Biol.* **2019**, *15*, 830.
[16] T. A. Ngo, H. Dinh, T. M. Nguyen, F. F. Liew, E. Nakata, T. Morii, *Chem. Commun.* **2019**, *55*, 12428.
[17] C. M. Niemeyer, T. Sano, C. L. Smith, C. R. Cantor, *Nucleic Acids Res.* **1994**, *22*, 5530.
[18] N. M. Green, *J. Biochem.* **1963**, *89*, 599.
[19] H. Yan, S. H. Park, G. Finkelstein, J. H. Reif, T. H. LaBean, *Science* **2003**, *301*, 1882.
[20] D. E. Lopatin, E. W. Voss, *Biochemistry* **1971**, *10*, 208.
[21] Y. He, Y. Tian, A. E. Ribbe, C. Mao, *J. Am. Chem. Soc.* **2006**, *128*, 12664.
[22] K. J. Brayer, D. J. Segal, *Cell Biochem. Biophys.* **2008**, *50*, 111.
[23] E. Nakata, F. F. Liew, C. Uwatoko, S. Kiyonaka, Y. Mori, Y. Katsuda, M. Endo, H. Sugiyama, T. Morii, *Angew. Chem. Int. Ed.* **2012**, *51*, 242.
[24] E. Nakata, H. Dinh, T. A. Ngo, M. Saimura, T. Morii, *Chem. Commun.* **2014**, *51*, 1016.
[25] T. A. Ngo, E. Nakata, M. Saimura, T. Morii, *J. Am. Chem. Soc.* **2016**, *138*, 3012.
[26] T. M. Nguyen, E. Nakata, M. Saimura, H. Dinh, T. Morii, *J. Am. Chem. Soc.* **2017**, *139*, 8487.
[27] S. Zhang, E. Nakata, P. Lin, T. Morii, *Chem. Eur. J.* **2023**, *29*, e202302093.
[28] K. Nakamura, S. Mizushima, *J. Biochem.* **1976**, *80*, 1411–1422.
[29] N. K. Burgess, T. P. Dao, A. M. Stanley, K. G. Fleming, *J. Biol. Chem.* **2008**, *283*, 26748–58.
[30] A. Gautier, A. Juillerat, C. Heinis, I. R. Corrêa, M. Kindermann, F. Beaufils, K. Johnsson, *Chem. Biol.* **2008**, *15*, 128.
[31] J. Han, K. Burgess, *Chem. Rev.* **2010**, *110*, 2709–2728.

Manuscript received: December 17, 2024
Revised manuscript received: January 24, 2025
Accepted manuscript online: February 6, 2025
Version of record online: ■■, ■■

RESEARCH ARTICLE

A DNA origami was used as the internal skeleton of the liposomes to control the number and polarity of the modular adaptor-fused OmpF assembly in the membrane to achieve pH-responsive and size-selective permeability. This approach offers the potential to construct artificial compartments containing membrane proteins of defined number and polarity, allowing tunable substrate fluxes.

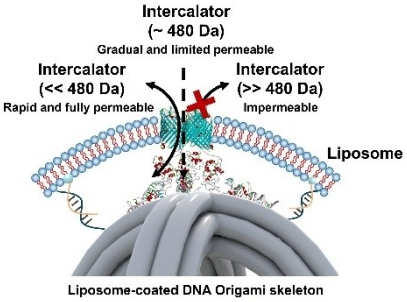

*Dr. S. Zhang, Dr. P. Lin, F. Komatsubara, Prof. E. Nakata, Prof. T. Morii**

1 – 10

A Practical Approach for Polarity and Quantity Controlled Assembly of Membrane Proteins into Nanoliposomes